Article:
Poulton, S.W., Krom, M.D. and Raiswell, R. (2004) A revised scheme for the reactivity of iron (oxyhydr)oxide minerals towards dissolved sulfide. Geochimica et Cosmochimica Acta, 68 (18). pp. 3703-3715. ISSN 0016-7037

https://doi.org/10.1016/j.gca.2004.03.012

White Rose
university consortium
Universities of Leeds, Sheffield & York

Revised Version submitted 11/03/04

A REVISED SCHEME FOR THE REACTIVITY OF IRON (OXYHYDR)OXIDE MINERALS TOWARDS DISSOLVED SULFIDE

Simon W. Poulton[1*], Michael D. Krom[2] and Robert Raiswell[2]

[1]Danish Center for Earth System Science, Institute of Biology, University of Southern Denmark, Campusvej 55, DK-5230 Odense, Denmark
Tel.: +45-65502745; E-mail: s.poulton@biology.sdu.dk
[2]School of Earth Sciences, University of Leeds, Leeds, LS2 9JT, UK

[*]Author to whom correspondence should be addressed.

Abstract

The reaction between dissolved sulfide and synthetic iron (oxyhydr)oxide minerals was studied in artificial seawater and 0.1 M NaCl at pH 7.5 and 25°C. Electron transfer between surface-complexed sulfide and solid phase Fe(III) results in the oxidation of dissolved sulfide to elemental sulfur, and the subsequent dissolution of the surface-reduced Fe. Sulfide oxidation and Fe(II) dissolution kinetics were evaluated for freshly precipitated hydrous ferric oxide (HFO), lepidocrocite, goethite, magnetite, hematite, and Al-substituted lepidocrocite. Reaction kinetics were expressed in terms of an empirical rate equation of the form:

$$R_i = k_i (\mathrm{H_2S})_{t=0}^{0.5} A$$

where R_i is the rate of Fe(II) dissolution (R_{Fe}) or the rate of sulfide oxidation (R_S), k_i is the appropriate rate constant (k_{Fe} or k_S), $(H_2S)_{t=0}$ is the initial dissolved sulfide concentration, and A is the initial mineral surface area. The rate constants derived from the above equation suggest that the reactivity of Fe (oxyhydr)oxide minerals varies over two orders of magnitude, with increasing reactivity in the order, goethite < hematite < magnetite << lepidocrocite ≈ HFO. Competitive adsorption of major seawater solutes has little effect on reaction kinetics for the most reactive minerals, but results in rates which are reduced by 65-80% for goethite, magnetite, and hematite. This decrease in reaction rates likely arises from the blocking of surface sites for sulfide complexation by the adsorption of seawater solutes during the later, slower stages of adsorption (possibly attributable to diffusion into micropores or aggregates). The derivation of half lives for the sulfide-promoted reductive dissolution of Fe (oxyhydr)oxides in seawater, suggests that mineral reactivity can broadly be considered in terms of two mineral groups. Minerals with a lower degree of crystal order (hydrous ferric oxides and lepidocrocite) are reactive on a time-scale of minutes to hours. The more ordered minerals (goethite, magnetite, and hematite) are reactive on a time-scale of

tens of days. Substitution of impurities within the mineral structure (as is likely in nature) has an effect on mineral reactivity. However, these effects are unlikely to have a significant impact on the relative reactivities of the two mineral groups.

1. INTRODUCTION

Iron (oxyhydr)oxide minerals are a major constituent of rocks and soils, and account for approximately 40-45% of the total iron content of sediments supplied to the global ocean (Poulton and Raiswell, 2002). The reductive dissolution of these minerals by hydrogen sulfide in organic-rich environments exerts a major control on dissolved sulfide profiles (e.g. Canfield, 1989; Canfield et al., 1992), and results in the release to solution of associated trace metals, organics, and ligands such as phosphate (e.g. Krom and Berner, 1981; Morse, 1994). The microbial generation of the dissolved sulfide required for this reaction is generally most rapid in the uppermost portion (commonly the top 10 cm) of organic-rich marine sediments (e.g. Jørgensen, 1977; Canfield, 1989; Canfield et al., 1993). However, the porewater distribution of dissolved sulfide is buffered in this zone by reaction with iron minerals (Canfield, 1989; Canfield et al., 1992). This occurs due to the oxidation of dissolved sulfide at the mineral surface, followed by release of the produced Fe(II) to solution and subsequent reaction with additional porewater sulfide to produce FeS (Pyzik and Sommer, 1981; Yao and Millero, 1996; Poulton, 2003). Thus this region is commonly characterized by low levels of dissolved sulfide and significant concentrations of dissolved iron (Canfield and Raiswell, 1991).

The extent to which iron minerals are able to control porewater sulfide distributions depends on the reactivity and abundance of the particular minerals present (Canfield, 1989; Canfield et al., 1992; Raiswell and Canfield, 1996). Iron minerals display a wide variability in terms of their reactivity towards dissolved sulfide, ranging from highly reactive Fe (oxyhydr)oxide minerals to essentially unreactive silicate Fe (Canfield et al., 1992; Dos Santos Afonso and Stumm, 1992; Raiswell and Canfield, 1996). Thus it is generally the availability of the most reactive Fe (oxyhydr)oxide minerals that ultimately controls the buffering of porewater dissolved sulfide.

The reaction mechanism between Fe (oxyhydr)oxides and dissolved sulfide has been the subject of a number of studies and is reasonably well-understood (Rickard, 1974; Pyzik and Sommer, 1981; Dos Santos Afonso and Stumm, 1992; Peiffer et al., 1992; Yao and Millero, 1996; Poulton, 2003). A variety of techniques have been used to assess reaction kinetics for various iron (oxyhydr)oxide minerals, including monitoring the formation of solid phase FeS (Rickard, 1974; Pyzik and Sommer, 1981), the oxidation of dissolved sulfide (Peiffer et al., 1992; Yao and Millero, 1996; Poulton et al., 2002; 2003; Poulton, 2003), and the dissolution of Fe(II) (Dos Santos Afonso and Stumm, 1992; Poulton, 2003). However no single study has employed a consistent approach to determine reaction kinetics for all the major iron (oxyhydr)oxides. Furthermore, it is the dissolution of Fe(II) from the (oxyhydr)oxide surface that ultimately controls the rate at which dissolved sulfide is fixed as FeS, and not the oxidation rate of sulfide (at the pH of most natural systems the kinetics for the latter are much faster; see Poulton, 2003).

Canfield et al. (1992) constructed the first reactivity scheme for the sulfidation of iron minerals, based on available literature data (a mixture of sulfide oxidation and Fe(II) dissolution rates) coupled with additional experiments. This scheme has been widely used and has proven to be an important aid to understanding the diagenetic behaviour of iron and sulfur (e.g. Gagnon et al., 1995; Haese et al., 1997; Hurtgen et al., 1999; Chambers et al., 2000; Morse et al., 2002; Krom et al., 2002). The direct application of reactivity schemes for the sulfidation of iron minerals to studies of natural systems is problematic, due to difficulties in ascertaining the precise mineralogy, surface areas and concentrations of the iron phases present, and due to differing competitive effects of dissolved species. Furthermore, Postma (1993) suggested that a reactive continuum exists for iron (oxyhydr)oxides in natural sediments, whereby reductive dissolution rates may be affected by surface area (which changes as the reaction progresses) and by the intrinsic reactivity of a particular mineral.

Nevertheless, kinetic evaluation of the sulfidation of Fe minerals under laboratory conditions remains an important tool for evaluating the behaviour of Fe and S in the environment. Thus it is perhaps surprising that no single study has attempted to provide a consistent approach to determine the reactivity of the major iron (oxyhydr)oxide minerals towards dissolved sulfide.

The reductive dissolution of iron (oxyhydr)oxides may be significantly affected by the adsorption of dissolved species at the oxide surface (Bondietti et al., 1993; Biber et al., 1994; Yao and Millero, 1996; Poulton, 2003; Poulton et al., 2003). The presence of adsorbed seawater solutes has been shown to decrease sulfide oxidation rates during reaction with freshly precipitated hydrous ferric oxide (Yao and Millero, 1996) and with 2-line ferrihydrite (Poulton et al., 2003). However, Poulton et al. (2003) demonstrated that reaction rates increase after the initial dissolution of the pre-adsorbed oxide surface due to exposure of fresh uncomplexed surface sites for reaction. Thus, the potential effect of competition between seawater solutes and dissolved sulfide for surface sites, may ultimately be of greater significance than pre-adsorption for the bulk reductive dissolution of Fe (oxyhydr)oxides. During reaction with 2-line ferrihydrite, the effect of competitive adsorption of major seawater solutes is negligible above pH 7.5, although reaction rates are significantly inhibited by competition with dissolved sulfate for available surface sites at lower pH (Poulton, 2003). However, the effect of competitive adsorption has not previously been determined for other iron (oxyhydr)oxides, and may be increasingly significant for the less reactive iron minerals.

In the present study we present a kinetic evaluation of the reactivity of a variety of Fe (oxyhydr)oxide minerals towards dissolved sulfide, including freshly precipitated hydrous ferric oxide (HFO), lepidocrocite (γ-FeOOH), goethite (α-FeOOH), hematite (α-Fe_2O_3) and magnetite (Fe_3O_4), in addition to Al-substituted lepidocrocite. These data are then combined with literature data for 2-line ferrihydrite (Poulton, 2003) to provide an internally-consistent scheme for the reactivity of the major naturally-occurring iron (oxyhydr)oxide minerals. We

additionally evaluate the effects of competitive adsorption of major seawater solutes and the effect of impurities within the crystal structure on the reactivity of the iron minerals.

2. SULFIDE-PROMOTED REDUCTIVE DISSOLUTION MODEL

The reaction between iron (oxyhydr)oxides and dissolved sulfide is a surface-controlled process and has been suggested to proceed via the following reaction sequence (dos Santos Afonso and Stumm, 1992):

(I) *Surface complex formation:*

$$>Fe^{III}OH + HS^- \underset{k_{-1}}{\overset{k_1}{\Leftrightarrow}} >Fe^{III}S^- + H_2O \quad (1)$$

(II) *Electron transfer:*

$$>Fe^{III}S^- \underset{k_{-et}}{\overset{k_{et}}{\Leftrightarrow}} >Fe^{II}S \quad (2)$$

(III) *Release of the oxidized product:*

$$>Fe^{II}S + H_2O \underset{k_{-2}}{\overset{k_2}{\Leftrightarrow}} >Fe^{II}OH_2^+ + S^{\cdot -} \quad (3)$$

(IV) *Detachment of Fe(II):*

$$>Fe^{II}OH_2^+ \overset{k_3}{\Rightarrow} \text{new surface site} + Fe^{2+} \quad (4)$$

Surface complex formation (Equation 1) is generally assumed to occur rapidly at the oxide surface (but see later), followed by electron transfer (Equation 2). The $S^{\cdot -}$ radical is then released (Equation 3) and rapidly reduces additional Fe(III) ions, to form higher oxidation state sulfur species. The Fe(II) produced at the oxide surface is then released to solution (Equation 4). In the case of sulfide oxidation by ferrihydrite, HFO and goethite, the

final oxidised sulfur product is dominantly elemental sulfur (Equation 5; Pyzik and Sommer, 1981; Yao and Millero, 1996; Poulton, 2003), and the Fe(II) released may react with additional dissolved sulfide to produce $FeS_{(s)}$ (Equation 6):

$$8{>}FeOH + 8S^{\bullet -} \Rightarrow S_8^0 + 8Fe^{2+} \quad (5)$$

$$Fe^{2+} + HS^- \Leftrightarrow FeS_{(s)} + H^+ \quad (6)$$

3. MATERIALS AND METHODS

3.1 Iron (oxyhydr)oxides

Synthetic lepidocrocite, goethite, hematite and magnetite were prepared according to the standard methods of Cornell and Schwertmann (1996). All chemicals were Analytical Reagent grade and all solutions were prepared in MilliQ water. Lepidocrocite was prepared by adjusting a 0.06 M $FeCl_2$ solution to pH 7 with NaOH to precipitate $Fe(OH)_2$. The precipitate was then oxidized with oxygen while maintaining the pH at 7 by the addition (via a pH-stat) of NaOH, and the final product was washed and dried. Goethite was prepared by the addition of 180 ml of 5 M KOH to 100ml of 1 M $Fe(NO_3)_3$. The resulting suspension was diluted to 2 l and heated at 70ºC for 60 h. The final precipitate was then washed and dried. Hematite was prepared by the addition of $Fe(NO_3)_3.9H_2O$ (to give a 0.02 M solution) to a preheated (98ºC) 0.002 M HCl solution. This solution was heated at 98ºC for 7 days, and the precipitate was then washed and dried. Magnetite was prepared by the slow addition of 240 ml of a 3.33 M KOH/0.27 M KNO_3 solution to a 0.3 M $FeSO_4$ solution (560 ml) preheated to 90ºC. The suspension was heated for 1 h with constant stirring, and the resulting precipitate washed and dried. The minerals were characterized using a Phillips PW1050 XRD with Cu Kα radiation.

Freshly precipitated hydrous ferric oxide was prepared by the addition of 0.1 M $FeCl_3$ to MilliQ water to give a required iron concentration. Precipitation of HFO was induced by the addition of 1 M NaOH to give a final pH of 7.5 (Crosby et al., 1983). Sulfidation experiments with HFO were then performed immediately, following degassing to remove oxygen.

Aluminium-substituted lepidocrocite minerals were prepared according to the method of Schwertmann and Wolska (1990). The pH of a 0.1 M $FeCl_2/Al(NO_3)_3$ solution was adjusted to 8.0 with NH_3/NH_4Cl (0.2 M NH_3 + 0.2 M NH_4Cl). The $FeCl_2/Al(NO_3)_3$ solutions were prepared to give lepidocrocites with 5% and 10% Al substitution. The solution was then oxidised by the addition of oxygen gas at a constant flow rate. During oxidation the solution was rapidly stirred with a magnetic stirrer, and the pH was maintained at a constant 8.0 ± 0.05 by the addition (via a pH-stat) of 1 M NH_3. After 3 hr the precipitate was washed and dried.

Surface area was measured by the multi-point BET method (using a Beckman/Coulter SA 1300 analyser with a Beckman/Coulter SA-PREP outgasser unit). Surface areas were determined as 61.4 $m^2\ g^{-1}$ for lepidocrocite, 122 $m^2\ g^{-1}$ for lepidocrocite with 5% Al, 172 $m^2\ g^{-1}$ for lepidocrocite with 10% Al, 36.5 $m^2\ g^{-1}$ for goethite, 2.5 $m^2\ g^{-1}$ for hematite, and 2.7 $m^2\ g^{-1}$ for magnetite. We made no surface area measurement for freshly precipitated HFO, due to a likely decrease in surface area upon drying (see Davis and Leckie, 1978).

3.2 Kinetic experiments

The experimental procedure was similar to that employed in a previous investigation of the reaction between dissolved sulfide and 2-line ferrihydrite (Poulton, 2003). The reaction is pH dependent (Pyzik and Sommer, 1981; dos Santos Afonso and Stumm, 1992; Peiffer et al., 1992; Yao and Millero, 1996; Poulton, 2003), and a pH of 7.5 (representing a

typical porewater pH for organic-rich marine sediments) was chosen for the experiments. The initial conditions for each experiment are shown in Table 1. Stock sulfide solutions were prepared by dissolving rinsed $Na_2S.9H_2O$ crystals in N_2-purged water. The N_2 (99.999%) used in this study was further purified by passing through an Alltech oxygen trap and then an Alltech indicating oxygen trap. The experimental apparatus consisted of a 1 l air-tight glass vessel, into which a pH electrode and ports for sample removal, degassing, and deoxygenated HCl addition were inserted by gas-tight screw plugs. Experiments were performed in constantly stirred artificial seawater (prepared according to the recipe of Millero, 1986) or 0.1 M NaCl. The temperature was maintained at 25°C with a Techne water bath, and light was excluded from all experiments. An appropriate volume of stock sulfide solution was added to the deoxygenated (by degassing for 1 h) aqueous medium via an air-tight syringe. The solution was then adjusted to pH 7.5 by the addition of deoxygenated 0.1 M HCl, and the initial dissolved sulfide concentration was measured in triplicate. A known weight of iron mineral was degassed for 1 hr in 10 ml of MilliQ water in an air-tight glass chamber attached directly to the sampling port of the reaction vessel. The mineral slurry was then added to the vessel by changing the N_2 flow direction and opening the input valve. This process took approximately 2-5 s (note that the other ports on the vessel remained closed during this process and thus no $H_2S_{(g)}$ was flushed from the system) and then the input port was immediately closed. This ensured that the mineral slurry remained completely anoxic during addition to the reaction vessel. A longer degassing time (18 h) had no detectable effect on reaction kinetics or products (Poulton, 2003). During the experiment the pH was maintained at a constant 7.5 ± 0.05 by the addition (via a pH-stat) of deoxygenated 0.1 M HCl. By using this system, interferences with pH buffers were avoided. Samples were periodically removed from the reaction vessel with a syringe for immediate analysis of dissolved and solid phases.

3.3 Chemical analysis

A detailed description of the analytical techniques used in this study is given in Poulton (2003). In brief, dissolved and solid phase sulfur species (with the exception of dissolved sulfate) were analysed by standard spectrophotometric techniques, with appropriate pre-treatment to avoid potential interferences between different sulfur species (e.g. Chen and Morris, 1972; O'Brien and Birkner, 1977; Pyzik and Sommer, 1981). Dissolved sulfide was measured on filtered (0.2 μm) samples and total sulfide (i.e. dissolved plus $FeS_{(s)}$) was measured on unfiltered samples by the methylene blue method (Cline, 1969). Replicate measurements of a stock sulfide solution gave a mean of 1088 ± 12 μM (2σ, n = 8). Filtered (0.2 μm) samples were periodically analysed for thiosulfate, sulfite, and sulfate. Sulfite was measured as the *p*-rosaniline hydrochloride complex in formaldehyde solution (West and Gaeke, 1956). Thiosulfate was determined by the copper catalysed acid cyanolysis of thiosulphate to thiocyanate (Urban, 1961). Sulfate was measured in experiments performed in 0.1 M NaCl using a Dionex DX-100 Ion Chromatograph. Elemental sulfur was determined on unfiltered samples as the $FeSCN^{+}$ complex after cyanolysis in acetone (Bartlett and Skoog, 1954). Total oxidised sulfur was determined as the difference between the initial sulfide concentration and the total sulfide concentration (solid plus dissolved) measured at a particular time interval.

Dissolved Fe(II) and Fe(III) were measured by the revised ferrozine method of Viollier et al. (2000). Dissolved Fe(III) was below detection (<0.5 μM) in all experiments. Replicate determinations of a stock Fe(II) solution gave a mean of 7.1 ± 0.3 μM (2σ, n = 6). The formation of aqueous FeS may contribute significantly to the total dissolved Fe pool at pH ≥ 7 (Luther et al., 1996; Zhang and Millero, 1994). Luther et al. (1996) report that soluble FeS complexes dissociate below pH 7, releasing H_2S from solution. Thus $FeS_{(aq)}$ was measured as part of the dissolved Fe(II) pool after addition of the acidic ferrozine reagent.

Total solid phase Fe(II) was determined after dissolution in 1 N HCl (Lovley and Phillips, 1987; Fredrickson et al., 1998). The sample was immediately purged with N_2 to dispel H_2S. The Fe(II) sorbed to particles was measured following extraction in buffered (pH 7) 1 M $CaCl_2$ for 2 h (Heron et al., 1994). After addition of the $CaCl_2$ the samples were immediately purged with N_2 to dispel H_2S. Total solid phase and sorbed Fe(II) were measured using the ferrozine assay (Stookey, 1970). The reduced Fe present as amorphous iron monosulfide was determined from the analysis of solid phase sulfide, assuming a composition $Fe_{1.05}S$ (Berner, 1964; note that small variations in the assumed composition of FeS have little effect on calculated reaction kinetics).

4. RESULTS

4.1 Chemical Speciation

Figure 1 shows typical results for the formation of sulfur and iron(II) species during the oxidation of dissolved sulfide by lepidocrocite. Similar speciation characteristics were observed for all minerals, with the only significant difference being the overall rates of reaction. In all cases the major removal pathway for dissolved sulfide was as oxidized sulfur rather than as solid phase FeS (Figure 1a). Samples were periodically analyzed for oxidized sulfur species, and elemental sulfur was found to be the dominant oxidized sulfur product during the reaction with all minerals. Dos Santos Afonso and Stumm (1992) found dissolved sulfate to be the dominant product during the reaction of sulfide with hematite in 0.01 M $NaClO_4$. However, in our experiments with hematite (and all other minerals) we detected no dissolved sulfate, and our sulfur speciation results are thus more consistent with the majority of previous studies (e.g. Rickard, 1974; Pyzik and Sommer, 1981; Peiffer et al., 1992; Yao and Millero, 1996; Poulton, 2003).

The sum of the Fe(II) phases was approximately double the concentration of sulfide oxidized for each sample, consistent with the conservation of electrons during the oxidation

of sulfide to elemental sulfur. The dominant Fe phase observed on the time-scale of these experiments was surface-reduced Fe (Figure 1b). This pool is distinct from the sorbed Fe(II) pool, which corresponds to Fe(II) which has been released to solution and subsequently re-adsorbed at the oxide surface (see Poulton, 2003). The formation of $FeS_{(s)}$ was also a significant pool for Fe(II), but dissolved and sorbed Fe(II) were only minor components prior to complete removal of dissolved sulfide (Figure 1b).

4.2 Iron(II) dissolution and sulfide oxidation kinetics

The reductive dissolution of Fe(II) and the oxidation of dissolved sulfide at pH 7.5 can be expressed by an empirical rate equation of the form:

$$R_i = k_i \, (\mathrm{H_2S})^{a}_{t=0} A^{b} \qquad (7)$$

where R_i is the rate of Fe(II) dissolution ($d(Fe^{2+})_{diss}/dt$; R_{Fe}) or the rate of sulfide oxidation ($-d(H_2S)_{tot}/dt$; R_S), k_i is the appropriate rate constant (k_{Fe} or k_S), $(H_2S)_{t=0}$ is the initial concentration of dissolved sulfide, A is the initial mineral surface area, and a and b are the reaction orders with respect to $(H_2S)_{t=0}$ and A, respectively. Mineral surface area is often used as a parameter in laboratory dissolution studies, as it is the availability of reactive surface sites that commonly controls the overall reaction (e.g. Zinder et al., 1986; Hering and Stumm, 1990; Stumm and Wieland, 1990; Dos Santos Afonso and Stumm, 1992; Peiffer et al., 1992; Biber et al., 1994; Poulton, 2003). However, the direct measurement of surface areas for individual Fe (oxyhydr)oxide minerals in natural sediments cannot readily be achieved, and thus the reaction kinetics will also be evaluated in terms of the initial concentration of Fe(III) present (defined as (Fe^{3+})).

Figure 2 shows representative data for the reductive dissolution of iron (oxyhydr)oxides by dissolved sulfide. The total concentration of Fe(II) dissolved from the oxide surface was calculated as the sum of dissolved, sorbed and monosulfide iron. In order

to develop an internally-consistent scheme for the reactivity of iron (oxyhydr)oxide minerals, we applied the approach used previously for 2-line ferrihydrite (initial rate theory) to evaluate reaction kinetics (see Poulton, 2003). Reductive dissolution rates (R_{Fe}) for each experiment were obtained by regression analysis of the linear relationships evident between total dissolved Fe(II) and time (Figure 2). For the more reactive iron (oxyhydr)oxides, rates of sulfide oxidation decrease significantly as sulfide is removed from solution. In addition, an initial decrease in sulfide concentration occurs due to the pre-equilibrium adsorption step (Equation 1). Thus initial oxidation rates were determined by regression analysis of the initial linear phase of sulfide removal, for the data obtained after the start of the experiments (i.e. concentrations of dissolved sulfide at $t = 0$ were not included in the data treatment). All regression equations were applied over the region where the error on the slope was within 5%. The *y*-axis intercept of these regression lines gives an estimate of the sulfide available for reaction after the initial adsorption step, and these estimates were used as the initial dissolved sulfide concentration.

Logarithmic plots of sulfide oxidation and Fe(II) dissolution rates as a function of the initial concentration of solid phase Fe(III) are shown for each mineral in Figure 3. Experiments with lepidocrocite, goethite, magnetite and hematite were performed at the same initial sulfide concentration (1055 ± 32 μM), while experiments with HFO were performed at an initial sulfide concentration of 249 ± 3 μM. The slopes of the lines in Figure 3 suggest a first order reaction with respect to the initial Fe(III) concentration (and surface area), consistent with a surface-controlled process (Pyzik and Sommer, 1981; Dos Santos Afonso and Stumm, 1992; Peiffer et al., 1992; Yao and Millero, 1996; Poulton, 2003).

The reaction order with respect to initial dissolved sulfide concentration was determined at mineral concentrations of 178 mg l^{-1} for lepidocrocite, goethite, magnetite and hematite, and a solid-phase Fe(III) concentration of 29 mg l^{-1} for HFO. The slopes of the

trends in Figure 4a imply a square root dependency for the oxidation of sulfide on initial sulfide concentration. Figure 4b suggests that the dependency of Fe(II) dissolution on initial sulfide concentration also approximates to a square root order. However, there is also some suggestion that this approximation may mask a systematic variation in reaction order in relation to the specific surface area of each mineral, whereby the reaction order tends to progressively increase with relative surface area. Thus magnetite (surface area = 2.7 m^2 g^{-1}) and hematite (surface area = 2.5 m^2 g^{-1}) have reaction orders of 0.45 and 0.47 respectively, goethite (surface area = 36.5 m^2 g^{-1}) has a reaction order of 0.50, and lepidocrocite (surface area = 61.4 m^2 g^{-1}) has a reaction order of 0.55. In addition, Poulton (2003) determined a reaction order of 0.57 for ferrihydrite (surface area = 299 m^2 g^{-1}). However, the errors on these slopes are relatively large (Figure 4b) and additional experiments are required to assess the significance of these potential variations. Thus in the present study we have assigned a 0.5 order to describe the dependency of Fe(II) dissolution on sulfide concentration, but recognise that some variation may occur as a result of differences in relative surface area between different minerals.

Determination of the reaction orders with respect to substrate concentration (or surface area) and initial sulfide concentration allows the following rate expressions to be defined:

$$R_S = k_S(H_2S)_{t=0}^{0.5}A \quad (8a)$$

$$R_{Fe} = k_{Fe}(H_2S)_{t=0}^{0.5}A \quad (8b)$$

Table 2 lists the sulfide oxidation and Fe(II) dissolution rate constants obtained when R_i is expressed in M min^{-1}, $(H_2S)_{t=0}$ is expressed in terms of M, A is expressed in m^2 l^{-1}, and (Fe^{3+}) is expressed in M. Rate constants are derived in terms of both the initial solid phase Fe(III) concentration and the initial surface area, for experiments performed in seawater at pH 7.5. The surface area of undried freshly precipitated HFO has been estimated to be in the range

300-600 m^2 g^{-1} (see Davis and Leckie, 1978), and to aid comparison between different minerals these values have been used to estimate k_S and k_{Fe} for HFO.

The calculation of rate constants in terms of (Fe^{3+}) for the oxidation of dissolved sulfide suggests that the reactivity of Fe (oxyhydr)oxides varies over four orders of magnitude, with a relative increase in the order, hematite < magnetite < goethite << lepidocrocite << HFO (Table 2). This mineral reactivity trend is similar to that evident for the dissolution of Fe(II), with the exception that rates are relatively increased for magnetite ($Fe_2^{3+}Fe^{2+}O_4$) due to the additional dissolution of structural Fe(II) (Table 2). Derivation of k_S and k_{Fe} in terms of surface area decreases the variability in Fe (oxyhydr)oxide reactivity to approximately two orders of magnitude (Table 2). This also results in a change in the order of mineral reactivity to, goethite < hematite < magnetite << lepidocrocite ≈ HFO. For all minerals, the reductive dissolution of Fe(II) was considerably slower than the rate of sulfide oxidation at pH 7.5 (Table 2).

4.3 Al-substituted lepidocrocite

The effect of Al substitution on the rate constants, k_S and k_{Fe}, is shown in Figure 5. Increased substitution of Al into the mineral structure results in a progressive decrease in crystal size, and thus an increase in surface area (Taylor and Schwertmann, 1980; Fitzpatrick and Schwertmann, 1982; Schwertmann and Wolska, 1990). Thus to facilitate a direct comparison between the different lepidocrocites, the rate constants used in Figure 5 were calculated in terms of surface area, rather than (Fe^{3+}). The substitution of Al results in a progressive decrease in reaction rates; rates were 60-70% slower for lepidocrocite with 10% Al substitution, relative to pure lepidocrocite (Figure 5).

4.4 Competitive adsorption

The effect of competitive adsorption of major seawater solutes on the rate of oxidation of dissolved sulfide is shown in Figure 6 (similar relationships were evident for Fe(II) dissolution). At pH 7.5, seawater solutes have little effect on reaction kinetics for the most reactive minerals (i.e. HFO and lepidocrocite), which is consistent with previous studies of competitive adsorption during the reaction of dissolved sulfide with ferrihydrite (Poulton, 2003). However, competitive adsorption resulted in a significant decrease in reaction rates for goethite, magnetite, and hematite, with rates in seawater being reduced by 65-80% in comparison to rates in 0.1 M NaCl.

5. DISCUSSION

5.1 Controls on reaction kinetics

In this section we evaluate the importance of various parameters for controlling reaction rates for individual Fe (oxyhydr)oxides, and assess the factors that may exert some control on the observed range in mineral reactivity. It is well established that, for a given pH and temperature, reaction kinetics in the Fe (oxyhydr)oxide-sulfide system are dependent on dissolved sulfide concentration and mineral surface area (Pyzik and Sommer, 1981; Dos Santos Afonso and Stumm, 1992; Peiffer et al., 1992; Yao and Millero, 1996; Poulton, 2003). The surface area control apparently occurs simply due to an increase in the availability of reactive surface sites at higher initial surface areas.

The determination of a fractional order for the dependency of sulfide oxidation on dissolved sulfide (Equation 8) is consistent with previous studies performed under conditions where the oxide surface was not in excess (Pyzik and Sommer, 1981; Poulton, 2003). In the study by Pyzik and Sommer (1981), the total reduction rate of goethite (i.e. solid phase Fe^{2+} plus dissolved Fe^{2+}) was calculated by an electron balance based on the formation of oxidized sulfur species. Thus the goethite reduction rate essentially equates to double the

sulfide oxidation rate (given that elemental S was the dominant product), and hence provides support for the 0.5 order dependency of sulfide oxidation rate on initial sulfide concentration determined for all minerals in the present study. The fractional order has been suggested to arise due to saturation of the most reactive surface sites at relatively low mineral to dissolved sulfide ratios (Poulton, 2003). However, given the wide range in relative surface areas of the studied minerals, it is perhaps surprising that all Fe (oxyhydr)oxides display the same relationship (Figure 4a; Pyzik and Sommer, 1981), since minerals with a lower surface area would be expected to become saturated with respect to surface-complexed sulfide at lower initial concentrations of dissolved sulfide.

Further insight into the potential role of sulfide concentration on sulfide oxidation rates may be gained by modeling the extent of reduction of the oxide surface. In the following example we use experimental data obtained for lepidocrocite (Run 82, Table 2; Figure 1). After 30 minutes, approximately 510 μm of Fe(II) was associated with the lepidocrocite surface. Assuming a surface hydroxyl density for lepidocrocite in the range 1.68 to 8 nm^{-2} (see Cornell and Schwertmann, 1996 and refs. therein), and given that adsorption reactions are most likely to involve only singly coordinated OH groups (Cornell and Schwertmann, 1996), the number of reduced Fe monolayers at the lepidocrocite surface lies in the range 3 to 16. The reduction of sub-surface Fe(III) could occur due to diffusion of sulfide into micropores (which may be too small to permit entry by the relatively large N_2 molecules used to measure surface area). Sulfide complexation at the oxide surface is usually considered to be a fast pre-equilibrium step in the reaction mechanism (Dos Santos Afonso and Stumm, 1992), but in fact adsorption is likely to be initially rapid, followed by a slower adsorption stage due to diffusion into micropores or aggregates, or due to structural rearrangement of surface complexes (Torrent, 1991; Fuller et al., 1993). An alternative explanation for the reduction of bulk phase Fe(III), is that electron transfer between sub-

surface Fe(III) and inner sphere-complexed sulfide may occur (possibly analagous to the abiotic and biotic reduction of structural Fe(III) in clay minerals; e.g. Stucki and Lear, 1990; Kostka et al., 1999). It is possible that both of the above processes may be facilitated by higher concentrations of dissolved sulfide, potentially giving rise (in conjunction with the effects of surface saturation) to the fractional order dependency of sulfide oxidation rate on sulfide concentration observed for all minerals.

The processes discussed above may also exert an influence on the fractional order dependence on sulfide concentration observed for the reductive dissolution of iron (oxyhydr)oxides (Figure 4b). Our observation that the reductive dissolution of Fe (oxyhydr)oxides approximates to a square root order with respect to dissolved sulfide concentration (but may also show some variation as a function of relative mineral surface area; see earlier) is consistent with in situ studies of the reductive dissolution of magnetite (Canfield and Berner, 1987). It should be noted, however, that this relationship has only been demonstrated at pH 7.5, where the dissolution of the produced Fe(II) from the oxide surface is considerably slower than the oxidation of sulfide (Table 2; Poulton 2003). The magnitude of the difference between sulfide oxidation and Fe(II) dissolution rates is highly pH dependent (Poulton, 2003), because the rate at which Fe(II) is detached from the surface depends on the extent of protonation of the nearest attached oxide or hydroxide ion (surface protonation accelerates the reductive dissolution by causing a polarization and weakening of the metal-oxygen bonds; Zinder et al., 1986; Suter et al., 1991). Under conditions where the oxide surface is saturated with respect to complexed sulfide (as in the present study), Fe(II) dissolution may be restricted by a lack of available reactive surface sites for protonation. Such a restriction could lead to the square root order estimated for the influence of sulfide concentration on the reductive dissolution of Fe (oxyhydr)oxides. Other factors, including the probability that dissolution of surface-reduced Fe(II) is likely necessary before Fe(II) in

the bulk phase can be dissolved, and the potential restriction of Fe(II) dissolution due to surface precipitation of FeS and elemental S, may also contribute to the observed dependency of Fe(II) dissolution on dissolved sulfide concentration.

The fact that a large proportion of the reduced Fe remains associated with the oxide surface (on the time-scale of these experiments) has implications for the distribution of Fe(II) during sediment diagenesis. High concentrations of non-sulfidic particulate Fe(II) have been found in near-surface sediments from a variety of coastal marine settings (Thamdrup et al., 1994; Thamdrup and Canfield, 1996; Rysgaard et al., 1998). The origin of this iron phase is unknown (Thamdrup and Canfield, 1996), and may represent the non-dissolved oxide-associated Fe(II) evident in the current experiments. Further studies of natural sediments are required to determine the origin, diagenetic fate, and overall effect on reaction kinetics of this iron pool.

Previous studies of the reaction of Fe (oxyhydr)oxides with dissolved sulfide provide contrasting evidence for the relative importance of surface area and mineralogy to the overall range in mineral reactivity. In preliminary experiments under acidic conditions (pH 5), Dos Santos Afonso and Stumm (1992) found that mineral reactivity could be directly related to thermodynamic considerations (free energy). By contrast, Morse and Wang (1997) suggest that reactivity is largely controlled by surface area. In the present study, a wide variation in reactivity is apparent when rate constants are defined in terms of surface area (Table 2). This suggests that it is not solely mineral surface area that controls reactivity. However, some of the variability in reactivity may be accounted for by differing surface site densities and surface acidity constants for the different minerals. Surface complexation modeling may be used to evaluate the extent of formation of surface-complexed sulfide for different Fe (oxyhydr)oxide minerals, based on the density of surface sites, surface acidity constants, and equilibrium constants for the specific adsorption of chemical species (e.g. Dos Santos Afonso

and Stumm, 1992; Peiffer et al., 1992; Yao and Millero, 1996; Poulton, 2003). However, the application of such an approach to dissolution reactions is limited because surface complexation theory does not account for the kinetics of sorption reactions (see Poulton, 2003). In fact, a simple evaluation of the relatively small variations reported for the acidity constants and surface site densities of Fe (oxyhydr)oxides (see Cornell and Schwertmann, 1996 and refs. therein), suggests that these factors can only be of minor importance in terms of explaining the observed range in reactivity.

The effects of competitive adsorption of major seawater solutes may also account for some of the observed variability in mineral reactivity. Surface complexation modeling suggests that magnesium (adsorbed as the $>FeOMg^{+}$ complex) is the most likely seawater solute to have a significant effect on reaction rates at pH 7.5 (Poulton, 2003). Competitive adsorption may clearly exert an important influence on reaction rates for the less reactive Fe (oxyhydr)oxides (i.e. magnetite, goethite, hematite), but has little effect on the reactivity of HFO and lepidocrocite (Figure 6). This is likely to occur because dissolved sulfide is able to outcompete the major seawater solutes for available surface sites during the early stages of the reaction with HFO and lepidocrocite. The reductive dissolution of HFO and lepidocrocite is relatively rapid, and the fast generation of new surface sites appears to enable sulfide to continuously outcompete seawater solutes. By contrast, the slower rates of reaction observed for magnetite, goethite and hematite, allows greater competition between dissolved sulfide and seawater solutes for available surface sites. This may occur because seawater solutes may be more efficient at competing with dissolved sulfide during the slower adsorption stage (i.e. during diffusion into micropores or particle aggregates; see earlier), resulting in greater competition for surface sites with less reactive minerals.

A second possible explanation for the differing effects of competitive adsorption relates to the potential for seawater solutes to replace sulfide already adsorbed at the oxide

surface. Such a process could be increasingly prevalent during the longer experiments required to establish reaction kinetics for the less reactive minerals. However, dissolved sulfide is able to form an inner sphere complex with surface Fe(III) (Luther, 1990), and is thus expected to be tightly bound and unlikely to be easily replaced by seawater solutes (Cornell and Schwertmann, 1996). Therefore, the increased effect of competitive adsorption for the less reactive minerals is more likely due to competition with dissolved sulfide during the slower adsorption stage. However, consideration of the effects of competitive adsorption suggests that, in the absence of major seawater solutes, mineral reactivity still varies by 1-2 orders of magnitude (when expressed in terms of surface area).

The above discussion suggests that surface properties such as relative surface area, acidity constants, and surface site densities, in addition to the varying effects of competitive adsorption, cannot account for the wide variability in Fe (oxyhydr)oxide reactivity. Litter and Blesa (1992) suggest that the differing reactivities exhibited by hematite and magnetite during photodissolution may be due to variations in electron mobility between the different Fe oxide structures. Factors such as electron mobility, in addition to morphological characteristics affecting bond strength, also appear to exert a major control on reactivity during reductive dissolution by sulfide.

In Figure 7 we have adopted a similar approach to that of Dos Santos Afonso and Stumm (1992), and consider the importance of intrinsic mineral reactivity in terms of free energy. Although the experimental systems of the present study are far from equilibrium, this approach can be considered to provide a comparison between reaction rates and morphological characteristics (i.e. degree of crystal order). Free energy was calculated for the following dissolution reactions (assuming a formula $Fe(OH)_3$ for freshly precipitated HFO):

$$2Fe(OH)_3 + H_2S + 4H^+ \Leftrightarrow 2Fe^{2+} + S^0 + 6H_2O \quad (9)$$

$$2FeOOH + H_2S + 4H^+ \Leftrightarrow 2Fe^{2+} + S^0 + 4H_2O \quad (10)$$

$$Fe_2O_3 + H_2S + 4H^+ \Leftrightarrow 2Fe^{2+} + S^0 + 3H_2O \quad (11)$$

$$Fe_3O_4 + H_2S + 6H^+ \Leftrightarrow 3Fe^{2+} + S^0 + 4H_2O \quad (12)$$

The free energy values used for Equations 9-12 were averages of reported values (see Cornell and Schwertmann, 1996 and refs. therein). To alleviate complications due to the formation of $FeS_{(s)}$ and the continued association of Fe(II) with the oxide surface at pH 7.5, calculations were performed at pH 4 (where $FeS_{(s)}$ does not form and all the reduced Fe(II) is present as aqueous Fe^{2+}). The rate constants for the dissolution of Fe(II) were expressed in terms of surface area and relate to rates in 0.1 M NaCl. Thus the rate constants used account for the differing effects of competitive adsorption and the different relative surface areas of the minerals. The exact chemical formula for freshly precipitated HFO is unclear, and thus the precise stoichiometry of Equation 9 is unknown. Thus the regression line in Figure 7 does not include the data for HFO. Nevertheless, the data suggest that the intrinsic reactivity of Fe (oxyhydr)oxides is a direct function of the free energy for the dissolution reactions. This observation further highlights the contrasting effects of crystal order and mineral surface area on the biotic and abiotic reductive dissolution of Fe (oxyhydr)oxides. Initial bacterial reduction rates for different Fe (oxyhydr)oxides tend to show a linear dependence on the relative surface area of each mineral, regardless of the degree of crystal order (e.g. Roden, 2003). By contast, the abiotic reduction of Fe (oxyhydr)oxides is apparently strongly influenced by morphological characteristics.

5.2 Iron (oxyhydr)oxide reactivity scheme

The order of mineral reactivity determined when rate constants are expressed in terms of surface area (goethite < hematite < magnetite << lepidocrocite ≈ HFO; Table 2) is consistent with previous studies of both non-reductive dissolution (Cornell et al., 1974; Sidhu

et al., 1981) and reductive dissolution by ligands other than sulfide (Postma, 1993). Furthermore, the relative reactivity of goethite and hematite is commonly reversed when rates are considered in terms of mass, due to the lower surface area for synthetic hematite relative to goethite (Table 2; LaKind and Stone, 1989; Postma, 1993). Therefore, a scheme to evaluate the relative reactivity of different minerals during diagenesis would ideally be evaluated in terms of the surface area of specific minerals. However, due to the difficulties involved in determining mineral surface areas in natural sediments, it is more practical to evaluate reactivity in terms of the concentration of solid phase Fe(III). This is a valid approach because the techniques used to prepare synthetic Fe (oxyhydr)oxides result in minerals with a reasonable morphological similarity to those in nature (Schwertmann, 1985). Thus, natural HFO exhibits the largest surface area of all the Fe (oxyhydr)oxides (commonly 150-550 m^2 g^{-1}; Schwertmann and Fischer, 1973; Carlson and Schwertmann, 1981; Borggaard, 1983). By contrast, natural goethites have much lower surface areas than HFO, but considerably higher surface areas than those estimated for natural hematite (Bigham et al., 1978). Furthermore, Canfield and Berner (1987) estimated relative surface areas of around 0.05-0.1 m^2 g^{-1} for discrete grains of magnetite from various marine sediments. This is likely to be a minimum value for magnetite, as surface area estimates were based on the largest crystals and the assumption of spherical geometry. Thus the relative surface areas for natural Fe (oxyhydr)oxides are similar to those measured for the synthetic minerals used in the present study. Therefore, a reactivity scheme defined in terms of the concentration of Fe(III) in synthetic minerals can be considered broadly applicable to studies of natural sediments.

Table 3 reports half lives for the reductive dissolution of the Fe (oxyhydr)oxides (calculated for a dissolved sulfide concentration of 1000 μM). The half lives were calculated following the determination of R_{Fe} (Equation 8b), and these rates were used to calculate the

rate constant (k) for the dissolution of Fe(II) (Equation 13). Half lives were then calculated using Equation 14:

$$k = R_{Fe}/(Fe^{3+}) \quad (13)$$

$$t_{1/2} = \ln(2)/k \quad (14)$$

The half lives reported in Table 3 relate to initial reaction rates, and thus their applicability to the bulk reductive dissolution of Fe (oxyhydr)oxides is limited. Nevertheless, these half lives provide a convenient assessment of the relative variability in Fe (oxyhydr)oxide reactivity, and enable direct comparisons with existing reactivity schemes (e.g. Canfield et al., 1992; Raiswell et al., 1994). Thus Fe (oxyhydr)oxides can be considered to fall into two broad categories in terms of reactivity (Table 3). Minerals with a lower degree of crystal order (freshly precipitated HFO, ferrihydrite, and lepidocrocite) are reactive on a time-scale of minutes to hours, while the more ordered forms (goethite, magnetite and hematite) react on a time-scale of tens of days. Within the less ordered group of minerals, hydrous ferric oxides (i.e. freshly precipitated HFO and ferrihydrite) also exhibit a range in reactivity, dependent on the conditions of formation and subsequent history (Table 3).

Raiswell et al. (1994) report comparable half lives for the dissolution of Fe (oxyhydr)oxides at a sulfide concentration of 1000 μM (based on rate constants reported in Canfield et al. (1992) for sulfide oxidation and Fe(II) dissolution data from various sources). While the half lives reported in Table 3 are broadly similar to those given in Raiswell et al. (1994), there are some notable differences. Thus lepidocrocite is considerably more reactive towards dissolved sulfide than has previously been recognised (Raiswell et al. (1994) suggest a half life of < 3 days), and can be considered comparable in reactivity to hydrous ferric oxides. The previously reported half life for hematite (31 days) was based on sulfide oxidation data and thus overestimates the dissolution rate at pH 7.5 (c.f. Table 3).

The largest discrepancy between the present study and previous estimates of reactivity occurs for magnetite. Previous estimates were based on depth profiles of the concentrations of discrete magnetite separated from a variety of continental margin sediments (Canfield and Berner, 1987). Based on this approach, a half life of 105 yr was obtained (Canfield et al., 1992; Raiswell et al., 1994), in comparison to 72 days as determined in the present study (Table 3). This discrepancy likely occurs due to a combination of two factors. Firstly, in addition to occurring as discrete mineral grains, detrital magnetite is also likely to be associated with mineral surfaces in sediments (Poulton and Canfield, in review). Furthermore, fine-grained biogenic magnetite may be a significant component in anaerobic sediments (e.g. Stolz et al., 1986; Lovley et al., 1987). Both of these forms of magnetite were not separated by the physical extraction scheme of Canfield and Berner (1987) and thus the total dissolution rate of sediment magnetite was likely underestimated. Secondly, part of the difference in estimated reactivity arises due to the low surface area (0.05-1.0 $m^2\ g^{-1}$) of the large magnetite grains studied by Canfield and Berner (1987). When differences in surface area are taken into account, our data suggest that magnetite is approximately 50 times more reactive than has previously been recognised. However, the most significant observation remains the fact that natural fine-grained magnetite is likely to be similar in reactivity to natural goethite and hematite (Table 3).

In nature, the reactivity of Fe (oxyhydr)oxides may be affected by impurities substituted within the mineral structure. The effect of substitution on dissolution rates is variable, and dependent on the substituent (see Cornell and Schwertmann, 1996). Our data for Al-substituted lepidocrocite suggest that reactivity (when expressed in terms of surface area) decreases with increasing substitution (Figure 5). This is likely due to changes in bond strength, since M-O-Fe bonds are stronger than Fe-O bonds and are thus more resistant to protonation (Schwertmann, 1984; Cornell and Schwertmann, 1996). However, the overall

change in reactivity with increasing substitution is relatively small in comparison to the variability observed between different Fe (oxyhydr)oxides (c.f. Table 2; Figure 5). Furthermore, Al substitution influences crystal growth rate and results in a decrease in crystal size and thus an increase in relative surface area (Schwertmann, 1984). When the sulfide-promoted dissolution rates are expressed in terms of (Fe^{3+}) rather than surface area, half lives (for a dissolved sulfide concentration of 1000 μM) of 8.1 h and 8.7 h were obtained for 5% and 10% Al-substituted lepidocrocite, respectively. These values suggest that Al-substituted lepidocrocite actually dissolves faster than pure lepidocrocite ($t_{1/2}$ = 10.9 h) due to the increased surface area available for reaction. This observation, coupled with the relatively small effect of Al substitution on reaction kinetics, suggests that impurities in Fe (oxyhydr)oxides are unlikely to greatly affect the reaction scheme for Fe (oxyhydr)oxides proposed in Table 3. Thus it appears that Fe (oxyhydr)oxide reactivity in nature may be reasonably expressed in terms of the two broad categories of mineral reactivity outlined above.

6. CONCLUSIONS

1. The derivation of rate constants for the oxidation of sulfide and the dissolution of Fe(II) in seawater at pH 7.5, suggests that rates of sulfide oxidation are considerably faster than rates of Fe(II) dissolution. Thus, consistent with previous studies of the reaction between dissolved sulfide and ferrihydrite (Poulton, 2003), the majority of the produced Fe(II) remains associated with the oxide surface (on the time-scale of these experiments) during the reaction with all major Fe (oxyhydr)oxides.

2. Rate constants for the Fe (oxyhydr)oxide minerals range over 4 orders of magnitude when expressed in terms of (Fe^{3+}), and two orders of magnitude when expressed in terms of surface

area. This wide range in reactivity is consistent with previous studies of the reductive and non reductive dissolution of Fe (oxyhydr)oxides (Sidhu et al., 1981; Postma, 1993), although actual dissolution kinetics vary considerably for different dissolution reactions.

3. The effect of competitive adsorption of major seawater solutes on reaction rates at pH 7.5 is insignificant for the more reactive minerals (HFO and lepidocrocite), but results in rates which are reduced by 65-80% for goethite, magnetite, and hematite. The effect of competitive adsorption is due to the blocking of available surface sites for sulfide complexation, and is likely enhanced during the later, slower adsorption stage.

4. The combined evaluation of the effects of surface properties and competitive adsorption suggests that these factors cannot explain the observed range in Fe (oxyhydr)oxide reactivity. Intrinsic factors such as bond strength and electron mobility also apparently exert an important influence on reactivity.

5. The derivation of half lives for the reductive dissolution of the major Fe (oxyhydr)oxides suggests that reactivity can be broadly considered in terms of two mineral groups. Minerals with a lower degree of crystal order (hydrous ferric oxides and lepidocrocite) are reactive on a time-scale of minutes to hours. The more ordered minerals (goethite, magnetite, and hematite) are reactive on a time-scale of tens of days. Substitution of impurities within the mineral structure (as is likely in nature) has an effect on mineral reactivity. However, these effects are unlikely to significantly alter the relative reactivities of the two mineral groups.

Acknowledgements

This study was carried out with financial support from the Commission of the European Communities, Agriculture and Fisheries (FAIR) specific RTD programme CT98-4160. SWP

additionally acknowledges support from a Marie Curie Individual Fellowship (HPMF-CT-2002-01569). We thank Jack Middelburg and two anonymous reviewers for very helpful comments which have considerably improved this manuscript.

REFERENCES

Bartlett, J.K. and Skoog, D.A. (1954) Colorimetric determination of elemental sulfur in hydrocarbons. *Anal. Chem.* **26,** 1008-1011.

Berner, R.A. (1964) Iron sulfides formed from aqueous solution at low temperatures and atmospheric pressure. *J. Geol.* **72,** 293-306.

Biber, M.V., Dos Santos Afonso, M., and Stumm, W. (1994) The coordination chemistry of weathering: IV. Inhibition of the dissolution of oxide minerals. *Geochim. Cosmochim. Acta* **58,** 1999-2010.

Bigham, J.M., Golden, D.C., Buol, S.W., Weed, S.B., and Bowen, L.H. (1978) Iron oxide mineralogy of well-drained ultisols and oxisols: II. Influence on color, surface area, and phosphate retention. *Soil. Sci. Soc. Am. J.* **42,** 825-830.

Bondietti, G., Sinniger, J., and Stumm, W. (1993) The reactivity of Fe(III) (hydr)oxides: effects of ligands in inhibiting the dissolution. *Colloids Surf.* **79,** 157-174.

Borggaard, O.K. (1983) The influence of iron oxides on phosphate adsorption by soil. *J. Soil Sci.* **34,** 333-341.

Canfield, D.E. (1989) Reactive iron in marine sediments. *Geochim. Cosmochim. Acta* **53,** 619-632.

Canfield, D.E. and Berner, R.A. (1987) Dissolution and pyritization of magnetite in anoxic marine sediments. *Geochim. Cosmochim. Acta* **51,** 645-659.

Canfield, D.E. and Raiswell, R. (1991) Pyrite formation and fossil preservation. In *Taphonomy: Releasing the Data Locked in the Fossil Record* (ed. P.A. Allison and D.E.G. Briggs), pp. 337-387. Plenum Press.

Canfield, D.E., Raiswell, R., and Bottrell, S. (1992) The reactivity of sedimentary iron minerals toward sulfide. *Am. J. Sci.* **292,** 659-683.

Canfield, D.E., Thamdrup, B., and Hansen, J.W. (1993) The anaerobic degradation of organic matter in Danish coastal sediments: Iron reduction, manganese reduction, and sulfate reduction. *Geochim. Cosmochim. Acta* **57,** 3867-3883.

Carlson, L. and Schwertmann, U. (1981) Natural ferrihydrites in surface deposits from Finland and their association with silica. *Geochim. Cosmochim. Acta* **45,** 421-429.

Chambers, R.M., Hollibaugh, J.T., Snively, C.S., and Plant, J.N. (2000) Iron, sulfur and carbon diagenesis in sediments of Tomales Bay, California. *Estuaries* **23,** 1-9.

Chen, K.Y. and Morris, J.C. (1972) Kinetics of oxidation of aqueous sulfide by O_2. *Environ. Sci. Technol.* **6,** 529-537.

Cline, J.D. (1969) Spectrophotometric determination of hydrogen sulfide in natural waters. *Limnol. Oceanogr.* **14,** 454-458.

Cornell, R.M. and Schwertmann, U. (1996) *The Iron Oxides: Structure, Properties, Reactions, Occurrence and Uses.* VCH: Weinheim.

Cornell, R.M., Posner, A.M., and Quirk, J.P. (1974) Crystal morphology and the dissolution of goethite. *J. Inorg. Nucl. Chem.* **36,** 1937-1946.

Crosby, S.A., Glasson, D.R., Cuttler, A.H., Butler, I., Turner, D.R., Whitfield, M., and Millward, S.E. (1983) Surface areas and porosities of Fe(III) and Fe(II)-derived oxyhydroxides. *Environ. Sci. Technol.* **17,** 709-713.

Davis, J.A. and Leckie, J.O. (1978) Surface ionization and complexation at the oxide/water interface. II. Surface properties of amorphous iron oxyhydroxide and adsorption of metal ions. *J. Colloid Int. Sci.* **67,** 90-107.

Dos Santos Afonso, M. and Stumm, W. (1992) Reductive dissolution of iron(III) (hydr)oxides by hydrogen sulfide. *Langmuir* **8,** 1671-1675.

Fitzpatrick, R.W. and Schwertmann, U. (1982) Al-substituted goethite-an indicator of pedogenic and other weathering environments in South Africa. *Geoderma* **27,** 335-347.

Fredrickson, J.K., Zachara, J.M., Kennedy, D.W., Dong, H., Onstott, T.C., Hinmann, N.W., and Li, S.-M. (1998) Biogenic iron mineralization accompanying the dissimilatory reduction of hydrous ferric oxide by a groundwater bacterium. *Geochim. Cosmochim. Acta* **62,** 3239-3257.

Fuller, C.C., Davis, J.A., and Waychunas, G.A. (1993) Surface chemistry of ferrihydrite: Part 2. Kinetics of arsenate adsorption and coprecipitation. *Geochim. Cosmochim. Acta* **57,** 2271-2282.

Gagnon, C., Mucci, A., and Pelletier, E. (1995) Anomalous accumulation of acid-volatile sulfides (AVS) in a coastal marine sediment, Saguenay Fjord, Canada. *Geochim. Cosmochim. Acta* **59,** 2663-2675.

Haese, R.R., Wallmann, K., Dahmke, A., Kretzmann, U., Müller, P.J., and Schulz. H.D. (1997) Iron species determination to investigate early diagenetic reactivity in marine sediments. *Geochim. Cosmochim. Acta* **61,** 63-72.

Hering, J.G. and Stumm, W. (1990) Oxidative and reductive dissolution of minerals. In *Mineral-Water Interface Geochemistry, Rev. Mineral.* (ed. M.F. Hochella, A.F. White), vol.23, pp. 427-465.

Heron, G., Crouzet, C., Bourg, A.C.M., and Christensen, T.H. (1994) Speciation of Fe(II) and Fe(III) in contaminated aquifer sediments using chemical extraction techniques. *Environ. Sci. Technol.* **28,** 1698-1705.

Hurtgen, M.T., Lyons, T.W., Ingall, E.D., and Cruse, A.M. (1999) Anomalous enrichments of iron monosulfide in euxinic marine sediments and the role of H_2S in iron sulfide transformations: Examples from Effingham Inlet, Orca Basin, and the Black Sea. *Am. J. Sci.* **299,** 556-588.

Jørgensen, B.B. (1977) The sulfur cycle of a coastal marine sediment (Limfjorden, Denmark). *Limnol. Oceanogr.* **5,** 814-832.

Kostka, J.E., Wu, J., Nealson, K.H., and Stucki, J.W. (1999) The impact of structural Fe(III) reduction by bacteria on the surface chemistry of smectite clay minerals. *Geochim. Cosmochim. Acta* **63,** 3705-3713.

Krom, M.D. and Berner, R.A. (1981) The diagenesis of phosphorus in a nearshore marine sediment. *Geochim. Cosmochim. Acta* **45,** 207-216.

Krom, M.D., Mortimer, R.J.G., Poulton, S.W., Hayes, P., Davies, I.M., Davison, W., and Zhang, H. (2002) In-situ determination of dissolved iron production in recent marine sediments. *Aquat. Sci.* **64,** 282-291.

LaKind, J.S. and Stone, A.T. (1989) Reductive dissolution of goethite by phenolic reductants. *Geochim. Cosmochim. Acta* **53,** 961-971.

Litter, M.I. and Blesa, M.A. (1992) Photodissolution of iron oxides. IV. A comparative study on the photodissolution of hematite, magnetite, and maghemite in EDTA media. *Can. J. Chem.* **70,** 2502-2510.

Lovley, D.R. and Phillips, E.J.P. (1987) Rapid assay for microbially reducible ferric iron in aquatic sediments. *Appl. Environ. Microbiol.* **53,** 1536-1540.

Lovley, D.R., Stolz, J.F., Nord, G.L.Jr., and Phillips, E.J.P. (1987) Anaerobic production of magnetite by a dissimilatory iron-reducing microorganism. *Nature* **330,** 252-254.

Luther III, G.W. (1990) The frontier-molecular-orbital theory approach in geochemical processes. In *Aquatic Chemical Kinetics* (ed. W. Stumm), Wiley, NY, pp.173-198.

Luther III, G.W., Rickard, D.T., Theberge, S.M., and Oldroyd, A. (1996) Determination of metal (bi)sulfide stability constants of Mn^{2+}, Fe^{2+}, Co^{2+}, Ni^{2+}, Cu^{2+} and Zn^{2+} by voltammetric methods. *Environ. Sci. Technol.* **30,** 671-679.

Millero, F.J. (1986) The pH of estuarine waters. *Limnol. Oceanogr.* **31,** 839-847.

Morse, J.W. (1994) Interactions of trace metals with authigenic sulfide minerals-implications for their bioavailability. *Mar. Chem.* **46,** 1-6.

Morse, J.W. and Wang, Q. (1997) Pyrite formation under conditions approximating those in anoxic sediments: II. Influence of precursor iron minerals and organic matter. *Chem. Geol.* **57,** 187-193.

Morse, J.W., Gledhill, D.K., Sell, K.S., and Arvidson, R.S. (2002) Pyritization of iron in sediments from the continental slope of the northern Gulf of Mexico. *Aq. Geochem.* **8,** 3-13.

O'Brien, D.J. and Birkner, F.B. (1977) Kinetics of oxygenation of reduced sulfur species in aqueous solution. *Environ. Sci. Technol.* **11,** 1114-1120.

Peiffer, S., dos Santos Afonso, M., Wehrli, B., and Gächter, R. (1992) Kinetics and mechanism of the reaction of H_2S with lepidocrocite. *Environ. Sci. Technol.* **26,** 2408-2413.

Postma, D. (1993) The reactivity of iron oxides in sediments: A kinetic approach. *Geochim. Cosmochim. Acta* **57,** 5027-5034.

Poulton, S.W. (2003) Sulfide oxidation and iron dissolution kinetics during the reaction of dissolved sulfide with ferrihydrite. *Chem. Geol.* **202,** 79-94.

Poulton, S.W. and Canfield, D.E. (in review) Development of a sequential extraction procedure for iron: Implications for iron partitioning in continentally-derived particulates.

Poulton, S.W. and Raiswell, R. (2002) The low-temperature geochemical cycle of iron: From continental fluxes to marine sediment deposition. *Am. J. Sci.* **302,** 774-805.

Poulton, S.W., Krom, M.D., van Rijn, J., and Raiswell, R. (2002) The use of hydrous iron (III) oxides for the removal of hydrogen sulphide in aqueous systems. *Wat. Res.* **36,** 825-834.

Poulton, S.W., Krom, M.D., van Rijn, J., Raiswell, R., and Bows, R. (2003) Detection and removal of dissolved hydrogen sulphide in flow-through systems via the sulphidation of hydrous iron (III) oxides. *Environ. Technol.* **24,** 217-229.

Pyzik, A.J. and Sommer, S.E. (1981) Sedimentary iron monosulfides: Kinetics and mechanism of formation. *Geochim. Cosmochim. Acta* **45,** 687-698.

Raiswell, R. and Canfield, D.E. (1996) Rates of reaction between silicate iron and dissolved sulfide in Peru Margin sediments. *Geochim. Cosmochim. Acta* **60,** 2777-2787.

Raiswell, R. and Canfield, D.E. (1998) Sources of iron for pyrite formation in marine sediments. *Am. J. Sci.* **298,** 219-245.

Raiswell, R., Canfield, D.E., and Berner, R.A. (1994) A comparison of iron extraction methods for the determination of degree of pyritisation and the recognition of iron-limited pyrite formation. *Chem. Geol.* **111,** 101-110.

Rickard, D.T. (1974) Kinetics and mechanism of the sulfidation of goethite. *Am. J. Sci.* **274,** 941-952.

Roden, E.E. (2003) Fe(III) oxide reactivity toward biological versus chemical reduction. *Environ. Sci. Technol.* **37,** 1319-1324.

Rysgaard, S., Thamdrup, B., Risgaard-Petersen, N., Fossing, H., Berg, P., Christensen, P.B., and Dalsgaard, T. (1998) Seasonal carbon and nutrient mineralization in a high-Arctic coastal marine sediment, Young Sound, Northeast Greenland. *Mar. Ecol. Prog. Ser.* **175,** 261-276.

Schwertmann, U. (1984) The influence of aluminium on iron oxides. IX. Dissolution of Al-goethites in 6 M HCl. *Clay Min.* **19,** 9-19.

Schwertmann, U. (1985) Some properties of soil and synthetic iron oxides. In *Iron in Soils and Clay Minerals* (eds. J.W. Stucki, B.A. Goodman, and U. Schwertmann), Windsheim, Germany, pp.203-250.

Schwertmann, U. and Fischer, W.R. (1973) Natural 'amorphous' ferric hydroxide. *Geoderma* **10,** 237-247.

Schwertmann, U. and Wolska, E. (1990) The influence of aluminum on iron oxides. XV. Al-for-Fe substitution in synthetic lepidocrocite. *Clays Clay Min.* **38,** 209-212.

Sidhu, P.S., Gilkes, R.J., Cornell, R.M., Posner, A.M., and Quirk, J.P. (1981) Dissolution of iron oxides and oxyhydroxides in hydrochloric and perchloric acids. *Clays Clay Min.* **29,** 269-276.

Stolz, J.F., Chang, S-B.R., Kirschvink, J.L. (1986) Magnetotactic bacteria and single-domain magnetite in hemipelagic sediments. *Nature* **321,** 849-851.

Stookey, L.L. (1970) Ferrozine-a new spectrophotometric reagent for iron. *Anal. Chem.* **42,** 779-781.

Stucki, J.W. and Lear, P.R. (1990) Variable oxidation states of iron in the crystal structure of smectite clay minerals. In *Spectroscopic Characterization of Minerals and their Surfaces,* ACS Symposium Series 415, pp. 330-358.

Stumm, W. and Wieland, E. (1990) Dissolution of oxide and silicate minerals: Rates depend on surface speciation. In *Aquatic Chemical Kinetics* (ed. W. Stumm), pp. 367-400, Wiley, New York.

Suter, D., Banwart, S., and Stumm, W. (1991) Dissolution of hydrous iron(III) oxides by reductive mechanisms. *Langmuir* **7,** 809-813.

Taylor, R.M. and Schwertmann, U. (1980) The influence of aluminum on iron oxides. VII. Substitution of Al for Fe in synthetic lepidocrocite. *Clays Clay Min* **28,** 267-271.

Thamdrup, B. and Canfield, D.E. (1996) Pathways of carbon oxidation in continental margin sediments off Central Chile. *Limnol. Oceanogr.* **41,** 1629-1650.

Thamdrup, B., Fossing, H., and Jørgensen, B.B. (1994) Manganese, iron, and sulfur cycling in a coastal marine sediment, Aarhus Bay, Denmark. *Geochim. Cosmochim. Acta* **58,** 5115-5129.

Torrent, J. (1991) Activation energy of the slow reaction between phosphate and goethites of different morphology. *Aust. J. Soil Res.* **29,** 69-74.

Urban, P.J. (1961) Colorimetry of sulphur anions: I. An improved colorimetric method for the determination of thiosulphate. *Z. Anal. Chem.* **179,** 415-422.

Viollier, E., Inglett, P.W., Hunter, K., Roychoudhury, A.N., and Van Cappellen, P. (2000) The ferrozine method revisited: Fe(II)/Fe(III) determination in natural waters. *Appl. Geochem.* **15,** 785-790.

West, P.W. and Gaeke, G.C. (1956) Fixation of sulfur dioxide as disulfitomercurate(II) and subsequent colorimetric estimation. *Anal. Chem.* **28,** 1816-1819.

Yao, W. and Millero, F.J. (1996) Oxidation of hydrogen sulfide by hydrous Fe(III) oxides in seawater. *Mar. Chem.* **52,** 1-16.

Zhang, J. and Millero, F.J. (1994) Investigation of metal sulfide complexes in seawater using cathodic stripping square wave voltammetry. *Anal. Chim. Acta* **284,** 497-504.

Zinder, B., Furrer, G., and Stumm, W. (1986) The coordination chemistry of weathering: II. Dissolution of Fe(III) oxides. *Geochim. Cosmochim. Acta* **50,** 1861-1869.

Table 1 Initial conditions for each experiment. AS = artificial seawater. [1]Concentration determined in terms of Fe(III) as the precise mineral weight of in situ precipitated HFO is unknown. ND = not determined.

Run no.	Mineral	Mineral concentration (mg l^{-1})	Surface area (m^2 l^{-1})	Initial ΣS^{2-} (μM)	Aqueous medium
54	hematite	388	0.96	1048	0.1 M NaCl
55	hematite	388	0.96	1044	AS
56	lepidocrocite	356	21.9	1060	AS
57	goethite	356	13.0	1049	AS
58	goethite	178	6.5	1090	AS
59	goethite	89	3.3	1094	AS
60	lepidocrocite	178	10.9	657	AS
61	lepidocrocite	89	5.5	1062	AS
62	lepidocrocite	178	10.9	1073	AS
63	goethite	178	6.5	812	AS
64	goethite	267	9.8	1085	AS
65	hematite	178	0.44	1021	AS
66	goethite	178	6.5	230	AS
67	hematite	267	0.66	1038	AS
68	hematite	89	0.22	1066	AS
69	hematite	178	0.44	816	AS
70	magnetite	356	0.98	1076	AS
71	HFO	29[1]	ND	246	AS
72	hematite	178	0.44	971	AS
73	goethite	178	6.5	641	AS
74	hematite	178	0.44	567	AS
75	HFO	10[1]	ND	250	AS
76	HFO	62[1]	ND	249	AS
77	HFO	29[1]	ND	392	AS
78	HFO	29[1]	ND	48	AS
79	HFO	21[1]	ND	252	AS
80	magnetite	178	0.49	544	0.1 M NaCl
81	HFO	29[1]	ND	108	AS
82	lepidocrocite	178	10.9	502	0.1 M NaCl
83	goethite	178	6.5	517	0.1 M NaCl
84	magnetite	178	0.49	1045	AS
85	magnetite	178	0.49	544	AS
86	magnetite	267	0.73	1054	AS
87	magnetite	178	0.49	799	AS
88	magnetite	89	0.24	1012	AS
89	magnetite	178	0.49	247	AS
90	10% Al lepidocrocite	178	30.6	518	AS
91	5% Al lepidocrocite	178	21.7	505	AS
92	lepidocrocite	178	10.9	180	AS
93	lepidocrocite	178	10.9	358	AS
94	HFO	29[1]	ND	251	0.1 M NaCl

Table 2 Rate constants for the oxidation of sulfide and the reductive dissolution of Fe(II) in seawater at pH 7.5. n = number of experiments. [1]assuming a surface area in the range 300-600 $m^2\ g^{-1}$ (see text for details).

Mineral	k derived in terms of (Fe^{3+})		k derived in terms of A		n
	k_S ($mol^{-0.5}\ l^{0.5}\ min^{-1}$)	k_{Fe} ($mol^{-0.5}\ l^{0.5}\ min^{-1}$)	k_S ($mol^{0.5}\ l^{0.5}\ m^{-2}\ min^{-1}$)	k_{Fe} ($mol^{0.5}\ l^{0.5}\ m^{-2}\ min^{-1}$)	
HFO	9.66 ± 1.68	4.41 ± 0.45	$(0.9\text{-}1.7 \times 10^{-5})$[1]	$(4.3\text{-}8.6 \times 10^{-6})$[1]	7
Lepidocrocite	$1.8 \times 10^{-1} \pm 0.4 \times 10^{-1}$	$3.4 \times 10^{-2} \pm 0.6 \times 10^{-2}$	$3.4 \times 10^{-5} \pm 0.7 \times 10^{-5}$	$6.1 \times 10^{-6} \pm 1.0 \times 10^{-6}$	8
Goethite	$1.7 \times 10^{-3} \pm 0.1 \times 10^{-3}$	$2.4 \times 10^{-4} \pm 0.3 \times 10^{-4}$	$5.3 \times 10^{-7} \pm 0.2 \times 10^{-7}$	$7.3 \times 10^{-8} \pm 1.0 \times 10^{-8}$	7
Magnetite	$1.5 \times 10^{-3} \pm 0.1 \times 10^{-3}$	$3.2 \times 10^{-4} \pm 0.7 \times 10^{-4}$	$4.5 \times 10^{-6} \pm 0.3 \times 10^{-6}$	$1.0 \times 10^{-6} \pm 0.2 \times 10^{-6}$	7
Hematite	$7.8 \times 10^{-4} \pm 1.1 \times 10^{-4}$	$8.9 \times 10^{-5} \pm 1.1 \times 10^{-5}$	$4.1 \times 10^{-6} \pm 0.6 \times 10^{-6}$	$4.2 \times 10^{-7} \pm 0.7 \times 10^{-7}$	7

Table 3 Half lives ($t_{1/2}$) for the reductive dissolution of Fe (oxyhydr)oxides in seawater at pH 7.5. Data for magnetite is calculated with the inclusion of structural Fe(II). Half lives are for a dissolved sulfide concentration of 1000 μM. [1]Poulton (2003).

Mineral	$t_{1/2}$
Freshly precipitated HFO	5.0 mins
2-line ferrihydrite[1]	12.3 h
Lepidocrocite	10.9 h
Goethite	63 days
Magnetite	72 days
Hematite	182 days

Figure Captions

Figure 1 Sulfur (A) and iron (B) speciation during the reaction of dissolved sulfide with lepidocrocite (surface area = 10.9 m^2 l^{-1}) at pH 7.5.

Figure 2 Representative data for the dissolution of Fe(II) in seawater at pH 7.5 (goe = goethite; mag = magnetite).

Figure 3 Logarithmic plots of sulfide oxidation rates (R_s; A) and Fe(II) dissolution rates (R_{Fe}; B) as a function of initial solid phase Fe(III) concentration. Experiments were performed at pH 7.5 in seawater, with initial sulfide concentrations of 1055 ± 32 μM for lepidocrocite, goethite, magnetite, and hematite, and 249 ± 3 μM for HFO (see Table 1).

Figure 4 Logarithmic plots of sulfide oxidation rates (R_s; A) and Fe(II) dissolution rates (R_{Fe}; B) as a function of initial sulfide concentration. Experiments were performed at pH 7.5 in seawater, with initial mineral concentrations of 178 mg l^{-1} for lepidocrocite, goethite, magnetite, and hematite, and a solid-phase Fe(III) concentration of 29 mg l^{-1} for HFO (see Table 1).

Figure 5 Effect of Al substitution on the sulfide oxidation and Fe(II) dissolution rate constants (derived in terms of surface area) for lepidocrocite.

Figure 6 Effect of competitive adsorption of major seawater solutes on the rate of sulfide oxidation by different iron (oxyhydr)oxide minerals at pH 7.5. $k_{S(sea)}$ = sulfide oxidation rate constant in seawater, $k_{S(NaCl)}$ = sulfide oxidation rate constant in 0.1 M NaCl.

Figure 7 Rate constants for the dissolution of Fe(II) (k_{Fe} in $mol^{0.5}$ $l^{0.5}$ m^{-2} min^{-1}) in 0.1 M NaCl as a function of the free energy (kJ mol^{-1}) for the reactions given in Equations 9-12. Free energy was determined at pH 4; 25°C; [H_2S] = 1 mM. The regression line is plotted for the data excluding HFO. Error bars represent the standard deviations reported in Table 2, with the exception of the error bars for HFO, which represent the range in k_{Fe} obtained assuming a surface area of 300-600 m^2 g^{-1}. Errors in $-\Delta G$ were calculated based on the ranges in ΔG_f^0 reported by Schwertmann and Cornell (1996), but were within the size of the data points.

Figure 1 Sulfur (A) and iron (B) speciation during the reaction of dissolved sulfide with lepidocrocite (surface area = 10.9 $m^2 l^{-1}$) at pH 7.5.

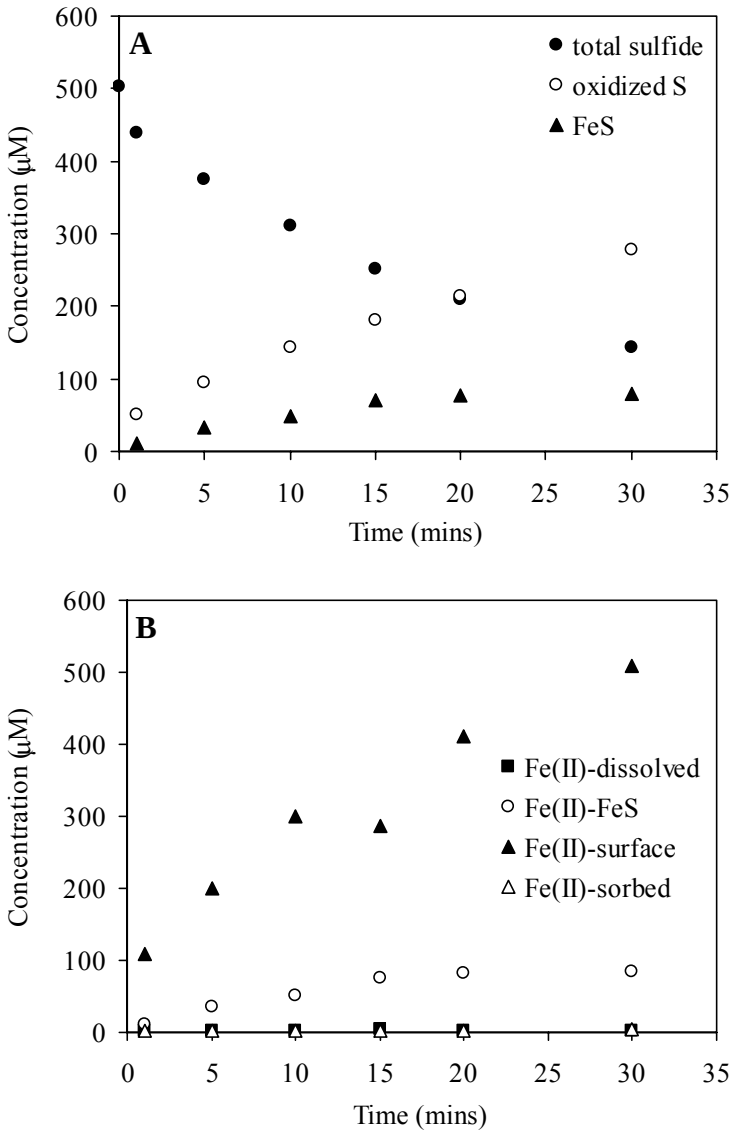

Figure 2 Representative data for the reductive dissolution of Fe(II) in seawater at pH 7.5 (goe = goethite; mag = magnetite).

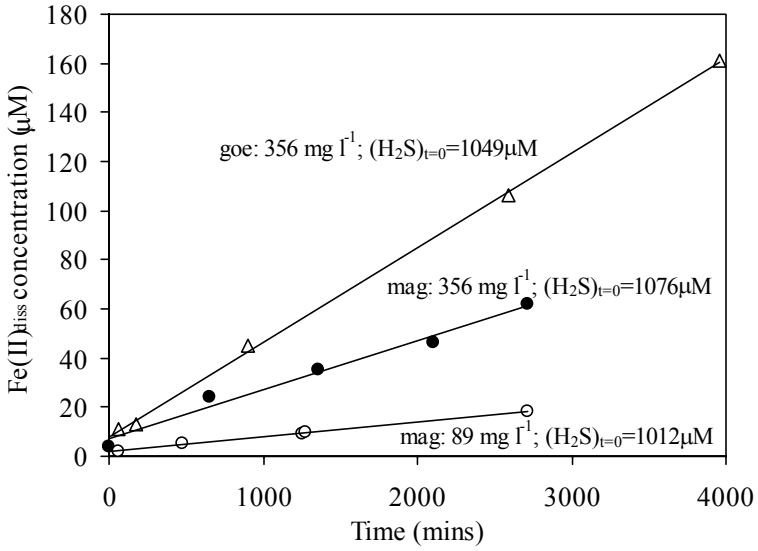

Figure 3 Logarithmic plots of sulfide oxidation rates (R_s; A) and Fe(II) dissolution rates (R_{Fe}; B) as a function of initial solid phase Fe(III) concentration. Experiments were performed at pH 7.5 in seawater, with initial sulfide concentrations of 1055 ± 32 μM for lepidocrocite, goethite, magnetite, and hematite, and 249 ± 3 μM for HFO (see Table 1).

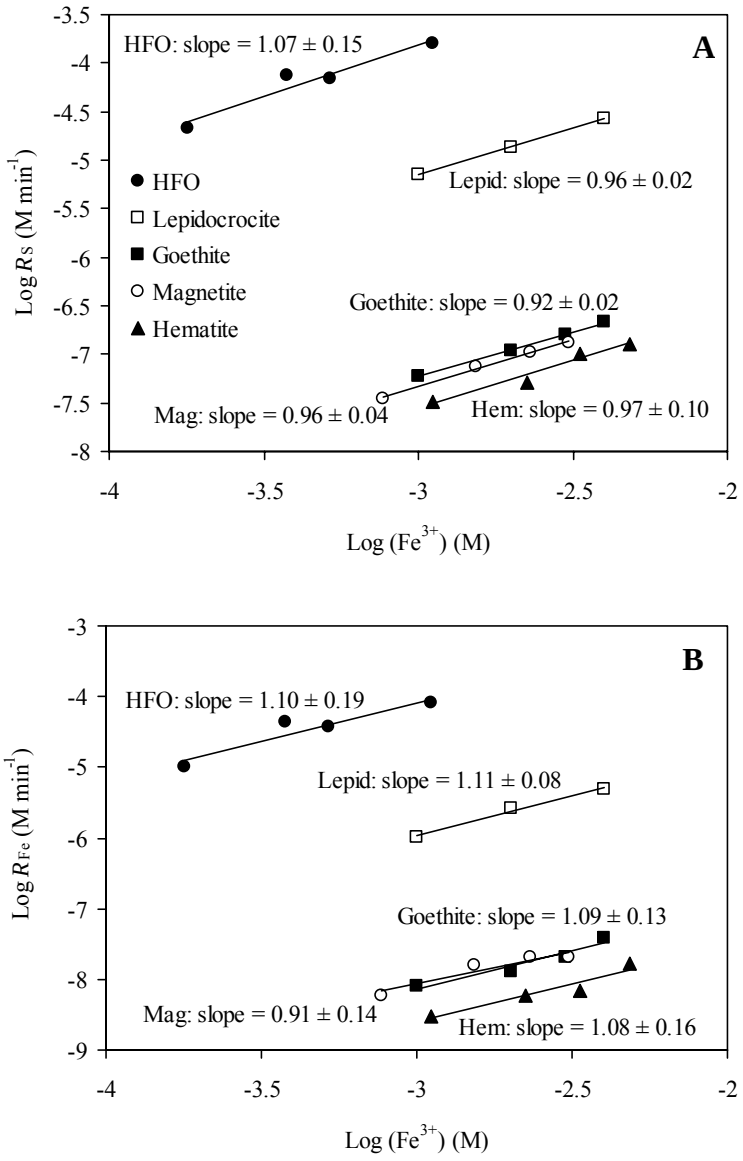

Figure 4 Logarithmic plots of sulfide oxidation rates (R_s; A) and Fe(II) dissolution rates (R_{Fe}; B) as a function of initial sulfide concentration. Experiments were performed at pH 7.5 in seawater, with initial mineral concentrations of 178 mg l^{-1} for lepidocrocite, goethite, magnetite, and hematite, and a solid-phase Fe(III) concentration of 29 mg l^{-1} for HFO (see Table 1).

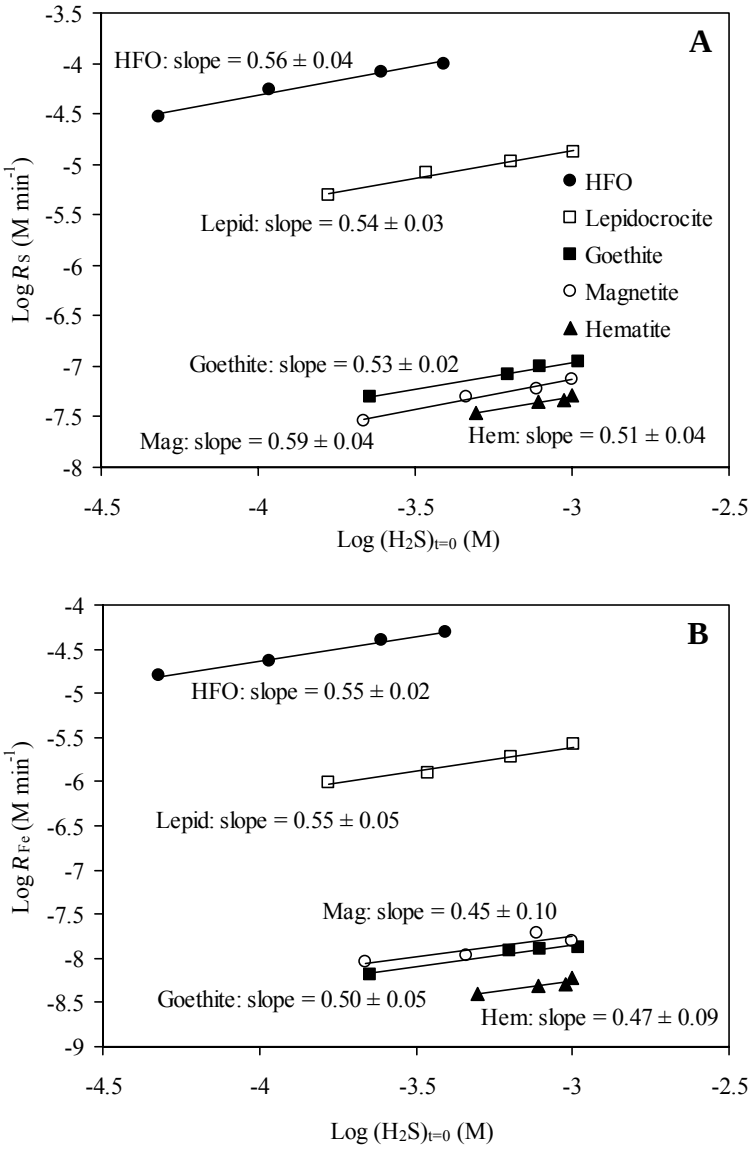

Figure 5 Effect of Al substitution on the sulfide oxidation and Fe(II) dissolution rate constants (derived in terms of surface area) for lepidocrocite.

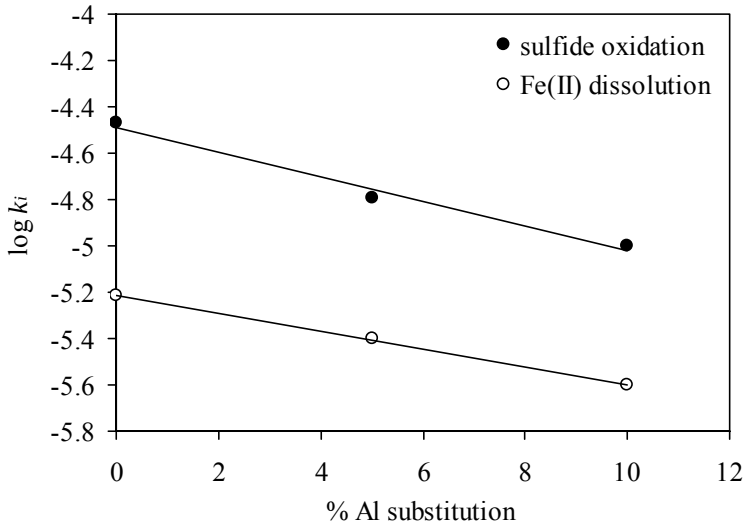
-4
-4.2
-4.4
-4.6
-4.8
-5
-5.2
-5.4
-5.6
-5.8
log ki
0
2
4
6
8
10
12
% Al substitution
sulfide oxidation
Fe(II) dissolution

Figure 6 Effect of competitive adsorption of major seawater solutes on the rate of sulfide oxidation by different iron (oxyhydr)oxide minerals at pH 7.5. $k_{S(sea)}$ = sulfide oxidation rate constant in seawater, $k_{S(NaCl)}$ = sulfide oxidation rate constant in 0.1 M NaCl.

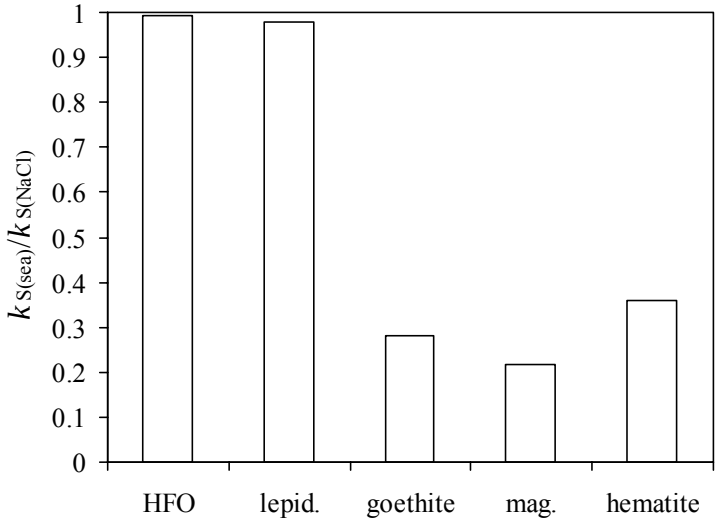

Figure 7 Rate constants for the dissolution of Fe(II) (k_{Fe} in $mol^{0.5}\ l^{0.5}\ m^{-2}\ min^{-1}$) in 0.1 M NaCl as a function of the free energy (kJ mol^{-1}) for the reactions given in Equations 9-12. Free energy was determined at pH 4; 25°C; $[H_2S]$ = 1 mM. The regression line is plotted for the data excluding HFO. Error bars represent the standard deviations reported in Table 2, with the exception of the error bars for HFO, which represent the range in k_{Fe} obtained assuming a surface area of 300-600 $m^2\ g^{-1}$. Errors in $-\Delta G$ were calculated based on the ranges in ΔG_f^0 reported in Schwertmann and Cornell (1996), but were within the size of the data points.